Energy spectrum of confined positively charged excitons in single quantum dots

M. R. Molas,[1,2,*] A. Wójs,[3,†] A. A. L. Nicolet,[2] A. Babiński,[1] and M. Potemski[2]

[1]*Faculty of Physics, University of Warsaw, ulica Pasteura 5, 02-093 Warszawa, Poland*

[2]*Laboratoire National des Champs Magnétiques Intenses, CNRS-UGA-UPS-INSA-EMFL, 25, avenue des Martyrs, 38042 Grenoble, France*

[3]*Department of Theoretical Physics, Wroclaw University of Science and Technology, Wybrzeże Wyspiańskiego 27, 50-370 Wrocław, Poland*

(Received 9 March 2016; revised manuscript received 25 October 2016; published 14 December 2016)

A theoretical model which relates the binding energy of a positively charged exciton in a quantum dot with the confinement energy is presented. It is shown that the binding energy, defined as the energy difference between the corresponding charged and neutral complexes confined on the same excitonic shell, strongly depends on the shell index. Moreover, we found that the ratio of the binding energy for positively charged excitons from the p and s shells of a dot depends mainly on the nearly perfect confinement inside the dot, which is due to the "hidden symmetry" of the multielectron-hole system. We applied the theory to the excitons confined to a single GaAlAs/AlAs quantum dot. The relevant binding energy was determined using microphotoluminescence and microphotoluminescence excitation magnetospectroscopy. We show that within our theory, the confinement energy determined using the ratio of the binding energy corresponds well to the actual confinement energy of the investigated dot.

DOI: 10.1103/PhysRevB.94.235416

I. INTRODUCTION

Semiconductor quantum dots (QDs) provide a unique environment to study fundamental properties of strongly interacting charge carriers [1–3]. The multitude of possible effects including direct and exchange Coulomb interactions and the resulting configuration mixing makes the energy spectrum of the complexes a complicated function of the confining potential and the relevant interactions. Both factors which depend on the QD size, shape, and composition must be taken into account to reliably describe the energy spectrum of excitons. Substantial efforts have been made to relate the morphology to experimentally addressable properties of carrier complexes confined in dots, i.e., the related photoluminescence (PL), which corresponds to emission, or the photoluminescence excitation (PLE), which corresponds to the absorption of light [4,5]. Among them the concept of "inverse engineering," which associates a specific order of emission lines due to particular excitonic complexes with a specific structure and composition of dots, can be acknowledged [6]. Due to that, we have recently shown that in natural InAs QDs the order results from a particular realization of the atomic species distribution [7].

The quest to relate some general properties of the QDs confining potential to the experimentally addressable features of carrier complexes in the dots also motivates this study. Our theoretical analysis shows that the ratio of the binding energy (BE) of the positively charged excitonic complexes related to the p and s shells of a strongly confined QD depends mainly on the confinement energy in the QD. We applied the model to our experimental results, confirming its validity in the GaAlAs/AlAs QDs formed in a GaAs/AlAs type-II bilayer.

II. THEORETICAL MODEL

We carried out the numerical calculations by exact diagonalization of model Coulomb Hamiltonians of the studied electron-hole (eh) complexes [an electron and a hole ($1e1h$) for the exciton and an electron and two holes ($1e2h$) for the positively charged exciton]. For simplicity, we assumed that the QD confinement is circular, strictly two-dimensional (i.e., of zero thickness), and laterally parabolic for both electrons and holes. Furthermore, we have assumed equal e and h oscillator length scales (i.e., identical corresponding electron and hole orbitals). This relies on nearly perfect (and thus spatially equal) confinement of both kinds of carriers inside the QD (such that both electrons and holes are entirely confined inside the same physical volume of the dot, with negligible orbital leakage into the barrier). Within our simple model this is expressed by equal ratios of electron and hole effective masses and confinement frequencies ($m_e\omega_e = m_h\omega_h$). This fulfils the condition of a "hidden symmetry" [8–10] based on mapping of the (real) eh system to a two-(pseudo)spin system with rotational invariance. It was demonstrated several times that the theoretical absorption spectra of a single QDs given by this model are in good agreement with excitonic complexes observed in PL experiments [11–15]. The main advantage of the harmonic oscillator model is the possibility to evaluate Coulomb matrix elements analytically, i.e., exactly and fast. The adjustable parameters are the oscillator length and energy (linked to the size and composition of the dot) and also the dielectric constant (controlling the strength of electron-electron interaction). The model is applicable to dots for which the single-electron energy spectrum is defined by the characteristic shell structure. These include various classes of natural dots. For example, the two-dimensional harmonic oscillator model has been shown [16–18] to capture dynamics in lens-shaped self-assembled dots in which the lateral motion adiabatically decouples from that in the normal direction, and an effective lateral confinement comes from the variable height of the dot. The neutral and positively charged exciton Hamiltonian matrices were expressed in the eh configuration bases, and we have included only a small number of the lowest electron and hole s, p, d, ... oscillator shells. For the present context of studying two particular optical transitions (between an exciton and vacuum and between a charged exciton and

*maciej.molas@gmail.com

†arkadiusz.wojs@pwr.edu.pl

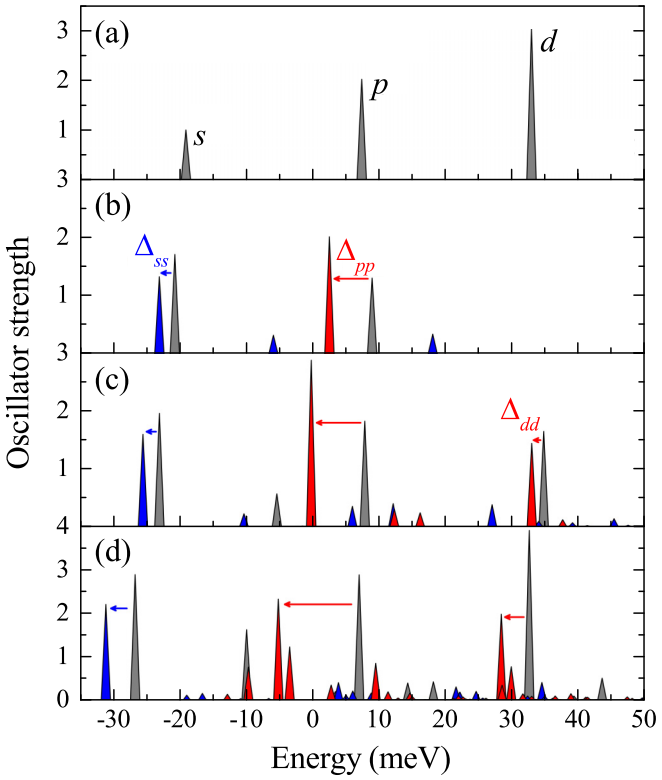

FIG. 1. Absorption spectra within the s, p, and d shells of a single QD parametrized by $\omega_e = 20$ meV and $\omega_h = 4$ meV in the absence of a magnetic field when (a) all intershell Coulomb scattering matrix elements are ignored and all Coulomb matrix elements within (b) two (s, p), (c) three (s, p, d), and (d) eight (s, p, d, ...) electron and hole shells are included. Note that (b) and (c) display absorption spectra limited to the lowest two and three shells, respectively, because all higher shells were excluded from the calculation. Gray and blue (red) peaks represent the resonances related to the neutral exciton ($1e_x1h_x$) and the singlet- (triplet-) spin state of the positively charged exciton ($1e_x1h_x1h_s$), respectively. The horizontal blue and red arrows indicate the magnitude of binding energy at the s, p, and d shells (Δ_{ss}, Δ_{pp}, and Δ_{dd}, respectively).

the hole in the s shell), only the subspaces with vanishing total orbital angular momentum $M = 0$ are important and have been considered. For the charged exciton, the total two-hole spin (singlet vs triplet) has been resolved in the diagonalization procedure. Finally, for each obtained neutral or charged exciton eigenstate we have also computed the oscillator strength for the relevant optical transition mentioned above: $1e1h \leftrightarrow$ vacuum and $1e2h \leftrightarrow h_s$.

Theoretical calculations were carried out using a model similar to that used previously, e.g., for emissions from multielectron dots [18]. The numerically determined absorption spectra for the neutral exciton as well as for the spin-singlet and the spin-triplet positively charged excitons are shown in Fig. 1. The energy scale in Fig. 1 excludes the band gap; that is, zero energy corresponds to an unconfined and noninteracting system of electrons and holes. Thus, for example, the energy shown for each excitonic (gray) peak contains the potential energy of each carrier with respect to the bottom of its (harmonic) potential well and the Coulomb interaction. The presented spectra were calculated with a particular choice of parameters: $\omega_e = 20$ meV and $\omega_h = 4$ meV (i.e., $\omega_e/\omega_h = m_h/m_e = 5$) and in the absence of magnetic field ($B = 0$ T). All material parameters (i.e., dielectric constant $\epsilon = 12.5$ and electron effective mass $m_e = 0.067m_0$) were taken as appropriate for GaAs. The Planck constant $\hbar$ is omitted here and in the following considerations for the sake of clarity. In the zero-order approximation only the electron-hole and the hole-hole intrashell Coulomb interactions were considered, with all intershell Coulomb scattering matrix elements neglected. The results of such an approach are displayed in Fig. 1(a). The spectra are identical for both complexes, with few peaks corresponding to the promotion of electrons from the successive $s, p, d, \ldots$ valence-band shells to the corresponding conduction-band shells. The peaks related to the shells are spaced roughly by the confining energy $\omega_e + \omega_h$ with oscillator strengths equal to the shell degeneracies.

Figures 1(b)–1(d) present the spectra obtained by including all Coulomb matrix elements within two, three, and eight electron and hole shells. Clearly, already the simple two-shell model, which includes the s and p shells, captures the essential behavior. Besides the known redistribution of excitonic oscillator strength from higher to lower peaks caused by intershell scattering, several points need to be noted about the trions: (i) Low-energy absorption adding to the s-shell hole an eh pair on the same lowest s shell creates only the spin-singlet charged exciton (blue peaks, including one marked "ss"). In contrast, higher-energy absorption adding an eh pair to different, higher shells predominantly creates the spin-triplet charged exciton (red peaks, including one marked "pp"). (ii) The energy difference Δ_{xx} between the corresponding neutral and charged exciton peaks ("ss," "pp," and "dd"), interpreted as the binding energy of an eh pair in different x shells ($1e_x1h_x$) to a charged complex comprising an eh pair in different x shells and a hole in the lowest s shell ($1e_x1h_x1h_s$), is not monotonic in the shell index $x = s, p, d, \ldots$. It does decrease with increasing $x = p, d, \ldots$ when absorption occurs in a different shell than that occupied by the initial electron ($x > s$), forming a spin-triplet charged exciton; it remains relatively low when absorption happens in the same shell ($x = s$), and a spin-singlet charged exciton is created. This exchange effect is a consequence of the (approximate) "hidden symmetry" in this system [8–10,19]. (iii) The magnitude of Δ_{xx} strongly increases with the number of the electron and hole shells included in the calculations [see Figs. 1(a)–1(c)].

In order to investigate further the effect of quantum confinement on the optical spectra of the neutral and positively charged excitons we performed the previously described analysis with three shells [compare Fig. 1(c)] for a broad range of the relevant parameters. To this end we determined the ratio R of the BE of the positively charged excitons on the p and s shells ($R = \Delta_{pp}/\Delta_{ss}$). The results of our calculations are illustrated in Fig. 2 in the form of a color-coded contour plot in intuitive $\omega_e + \omega_h$ and ω_e/ω_h coordinates. As can be appreciated in Fig. 2, the ratio R varies very little throughout most of the map. Moreover, for the experimentally justified case of $\omega_e/\omega_h > 1$ (corresponding to the usual $m_e/m_h < 1$) the contours go almost vertically in a broad range of the confinement energies. Particularly, in the case

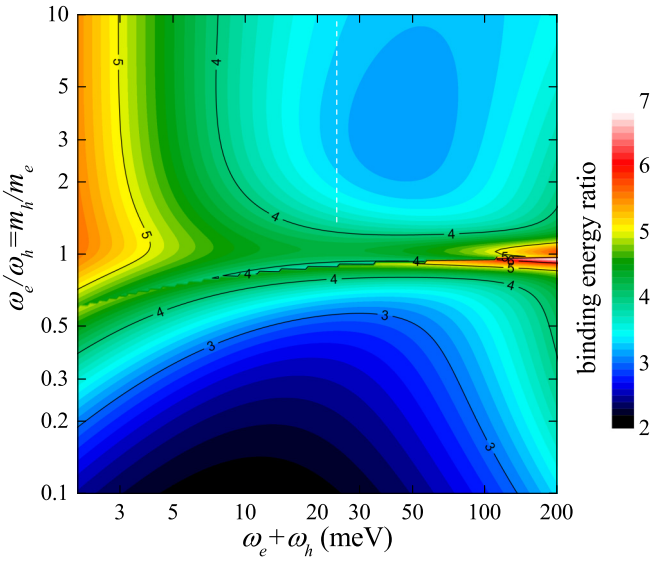

FIG. 2. Color-coded contour plot map of the binding energy ratio $R = \Delta_{pp}/\Delta_{ss}$ in coordinates $\omega_e + \omega_h$ and ω_e/ω_h.

of $\omega_e + \omega_h \approx 24$ meV, previously described in Fig. 1, $R = 3.5$ (see the white dashed line in Fig. 2).

III. SAMPLE AND EXPERIMENTAL SETUPS

The active part of the structure used in our study was intentionally designed as a GaAs/AlAs type-II bilayer ($d_{\mathrm{GaAs}} = 2.4$ nm, $d_{\mathrm{AlAs}} = 10$ nm) embedded between wide (100 nm) $Ga_{0.67}Al_{0.33}As$ barriers [20,21]. Previous research showed that the bilayer is not perfect in lateral directions: the Ga-rich inclusions, which can be seen as islands of $Ga_{1-x}Al_xAs$ ($x < 0.33$) replacing the original GaAs/AlAs bilayer, exist in this structure and possess all attributes of relatively strongly confined semiconductor QDs. These dots show remarkably low surface density, at the level of 10^5–10^6 cm^{-2}. Their emission spectra are dispersed in a wide energy range, 1.56–1.68 eV [22–28], due to the spread in the lateral extent of the confining potential.

Single-dot measurements have been carried out at liquid-helium temperature using a typical setup for the PL and PLE experiments. To detect the PL spectra, a tunable Ti:sapphire laser was set at $\lambda = 725$ nm to ensure the quasiresonant excitation conditions, i.e., to inject the *eh* pairs directly into QDs [29]. The PLE signal was obtained from the measured variations in the intensity of the emitted PL at a particular energy with changes of the excitation energy.

The setup was dedicated to measurements in an external magnetic field in the Faraday configuration with the aid of a superconducting magnet producing a field up to 9 T. The sample was located on top of an x-y-z piezo stage in a bath cryostat with optical access provided by a Y-shaped fiber equipped with a microscope objective (spot size around 1 μm^2) [30]. The laser light was coupled to one branch of the Y-shaped fiber, focused by the microscope objective, and the signal was detected from the second branch of the fiber by a 0.5-m-long monochromator equipped with a charge-coupled-device camera.

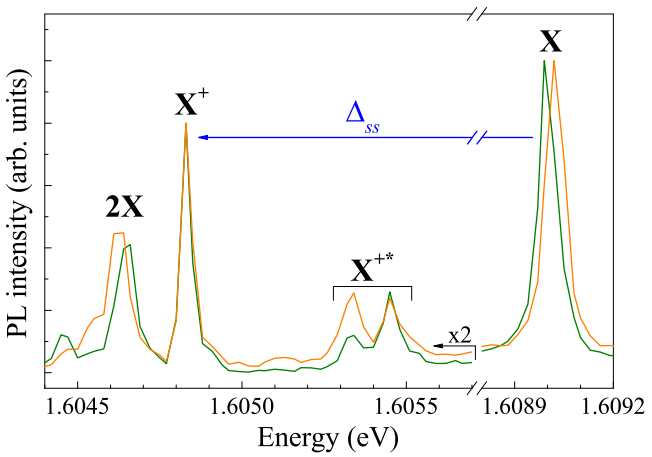

FIG. 3. The PL spectra of a single GaAlAs QD recorded for two perpendicular linear polarizations oriented along the crystallographic directions [110] (orange curve) and [1$\bar{1}$0] (green curve).

IV. EXPERIMENTAL RESULTS AND DISCUSSION

In order to experimentally verify the model and to find R for a particular QD, single-dot PL and PLE spectra must be collected and analyzed. Moreover, as shown later, the PLE measurements in magnetic field need to be performed in order to identify neutral and positively charged excitons originating from the absorption between p shells of the conduction and valence bands.

The BE of the positively charged exciton at the ground s shell Δ_{ss} is defined as the energy difference between the emission lines attributed to the singlet state of the positively charged exciton (X^+) and to the neutral exciton (X). The results of polarization-sensitive PL measurements on the investigated QD are shown in Fig. 3. It was found that both the X and the 2X emission lines split into two linearly polarized components (the magnitude of splitting was equal to about 23 μeV), which is characteristic of neutral excitonic complexes. The excitation-power-dependent measurements confirmed that the former line corresponds to recombination of a neutral exciton ($1e_s1h_s$), while the latter results from the optical recombination of a neutral biexciton ($2e_s2h_s$). The fine-structure splitting of the neutral exciton and biexciton is a consequence of the *eh* exchange interaction in the dot characterized by the anisotropic potential, and it was intensively studied in the literature [31–35].

The X^+ line did not split, which is characteristic of a singlet state of a charged exciton. The attribution of the line to the spin-singlet state of a singly, positively charged exciton was the topic of previous studies [27,36] and will not be discussed here. The complex consists of an s-shell electron and two s-shell holes ($1e_s2h_s$). There is no fine structure splitting of the X^+ line because the *eh* exchange interaction influences neither the initial state (where the two holes form a closed shell) nor the final state (only one hole left) [34]. One must note that the presence of the emission lines due to different charge states of a QD (neural and positively charged) under quasiresonant excitation is characteristic of spectra measured over some time (5 s in our case) and results from charge fluctuations in the structure [26].

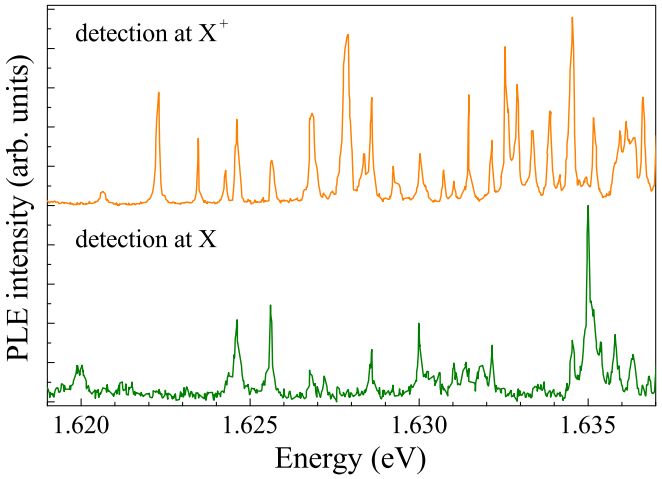

FIG. 4. The PLE spectra detected on the X (green curve) and X^+ (orange curve) emission lines of a single GaAlAs QD. The spectra are normalized to the most intense peaks and shifted for clarity.

The BE of the positively charged exciton at the s shell (of an s-shell exciton to the s-shell hole) determined from the analysis for the investigated QD is $\Delta_{ss} \approx 4$ meV.

For the sake of completeness yet another emission line (X^{+*}) present in the spectrum should be addressed. It is ascribed to the spin-triplet state of a singly, positively charged exciton ($1e_s1h_s1h_p$), and its fine structure results from the eh and hole-hole exchange interaction (see Ref. [36] for details).

More complicated is the determination of the BE of the positively charged exciton at the p shell Δ_{pp}. The BE is defined as the difference between the energies of the triplet state of the positively charged exciton ($1e_p1h_p1h_s$) and the neutral exciton in the excited state ($1e_p1h_p$). These states do not usually recombine radiatively due to their fast relaxation to the spin singlet of a positively charged exciton and the ground state of the neutral exciton. They should, however, contribute to the resonances in the PLE spectra of the charged and neutral excitons measured, respectively, at the X and X^+ emission lines. The PLE spectra are presented in Fig. 4.

There are several resonances in the spectra which cannot be directly attributed to the sought excited states of the neutral and positively charged excitons. It is not obvious at the moment what the origin of the multitude of resonances is. The symmetry breaking and the resulting mixing with higher-energy bands could be a possible origin of the resonances [37]; however, no solid explanation of the effect can be proposed. As a plethora of resonances does not facilitate their attribution to particular excitonic configurations, we investigated their evolution in magnetic field applied in the Faraday configuration. As we know from previous experiments on the investigated dots, several shells (s, p, d) are available to excitonic complexes confined in them [23,27]. The single-particle electronic state of a particle confined in the parabolic potential is expected to follow the Fock-Darwin structure [38,39]. Previous experiments on QDs showed that the characteristic evolution is also reproduced by the energy structure of the excitonic states [13,14]. Particularly, as a consequence of the diamagnetic shift, the s-shell-related complexes experience a blueshift in magnetic field. In contrast, the energy of a complex related to the excited states associated with the p shells, which are of interest to us, is supposed to lower its energy with magnetic field (which results from Zeeman interaction of the orbital momentum of the complex with the magnetic field). The results of the measurements are shown in Fig. 5. As the energies of the positively charged exciton and the neutral exciton shift diamagnetically in magnetic field and split due to Zeeman interaction, the energy scales in both Figs. 5(a) and 5(b) are relative to the energy of the X emission line at zero magnetic field. In the following we address both results.

The PLE spectra of the neutral exciton [see Fig. 5(a)] can be divided into two energy ranges: above and below ~21 meV. In the low-energy range, all resonant peaks show the same type of the magnetic field evolution. Their energies increase with magnetic field, which is characteristic diamagnetic behavior of carriers and complexes with zero-orbital momentum. Such an evolution relates the resonances to the s shell of the investigated dot [14]. We can observe them at a relative energy higher than approximately 10 meV, and the energy difference between them is only around 1–2 meV. The observed resonances also split in magnetic field due to Zeeman spin interaction. It can be noted that a similar s-type evolution of the resonances in the range below ~20 meV is also characteristic of the magneto-PLE spectra of the X emission line measured on two other QDs (see Fig. 1 of the Supplemental Material [40]). A complicated picture of the splitting of particular resonances observed in particular polarizations of the ground state makes the full analysis of the effect quite a complicated task. The attribution of excited electron states is excluded because the observed energy distance between the s- and p-shell emissions in the PL spectra is around 14 meV, which is related mainly to the energy separation between the electron levels (for details see Ref. [28]). We provisionally ascribed the resonances to absorption processes occurring between the excited hole levels, e.g., the p, d, ... shells, and the ground electron level, the s shell [27,41,42]. Such an attribution would explain the diamagnetic shift of the resonances. At high energies, the observed pattern of resonant peaks becomes extremely complex, and the peaks can be hardly followed with the magnetic field. In our opinion some additional transitions involving phonon replicas could be responsible for resonances in this energy range. Nevertheless, there are resonances observed in that energy range which lower their energies with magnetic field which characterize the p-shell-like evolution. The lowest-energy resonance of that behavior can be appreciated following the structure which originates around ~26 meV at $B = 0$ T. We ascribed this peak to the excited state of the neutral exciton, labeled X^* ($1e_p1h_p$), involving the absorption of an electron from the p-shell level in the valence band to the p-shell level in the conduction band. As could be expected, the X^* transition (peak at ~1.635 eV in the bottom trace of Fig. 4) is seen as the most pronounced resonance in the PLE spectra of the neutral exciton ground state, measured at $B = 0$. Moreover, X^* is the only transition which shows the traces of the p-like character in the magneto-PLE spectra [see Fig. 5(a), resonance at 26 meV in the zero-field spectrum]. All other lower-in-energy resonances show a clear s-like behavior, which now also can be seen in the spectra

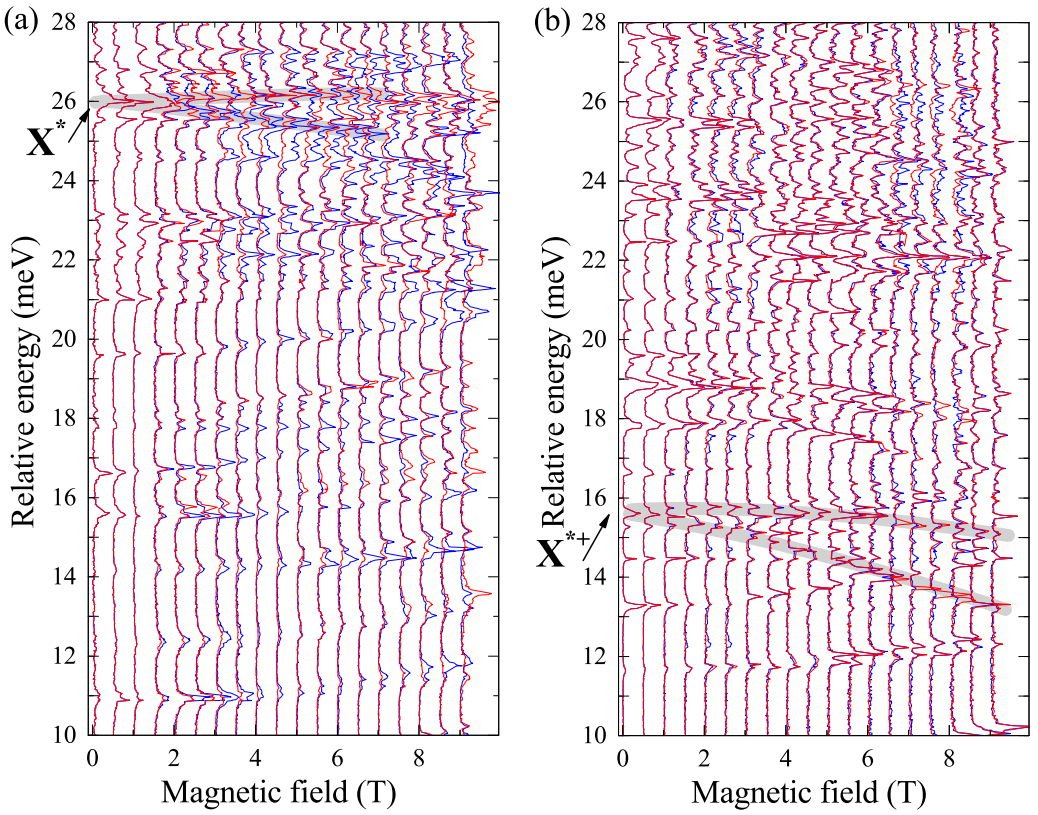

FIG. 5. The magnetic-field evolution of PLE spectra detected on the (a) X and (b) X^+ emission lines. The red and blue curves indicate the σ_+- and σ_--polarized components of the lines, on which the PLE spectra were measured. The scale of the vertical axis is set by the energy relative to the X emission line at 0 T. The spectra are normalized to the most intense peaks and shifted for clarity. Gray lines are guides to the eye.

measured on two other dots (see Fig. 1 of the Supplemental Material [40]).

In the case of magnetic-field evolution of PLE spectra of the spin-singlet state of the positively charged exciton, presented in Fig. 5(b), there are also two types of resonances: s- and p-shell-like. The observation of the s-shell-like magnetic-field dependence might also be ascribed to the transitions between the excited hole levels, e.g., the p, d, ... shells, and the ground electron level, the s-shell, but in the presence of an additional hole [27,41,42]. Moreover, the peak, appearing around $\sim$15.5 meV at $B = 0$ T, lowers its energy with the magnetic field. As a consequence of the p-shell-like evolution, this peak has been attributed to the absorption process of the excited state of the positively charged exciton, labeled X^{*+} ($1e_p1h_p1h_s$), which involves the absorption process of an electron from the p-shell level in the valence band to the p-shell level in the conduction band in the presence of an extra hole on the s shell (see Refs. [27,43] for details). In support of our assignment are additional experimental data measured on two other dots (magneto-PLE) and presented in the Supplemental Material [40] (Fig. 2). The X^{*+} resonance can be clearly recognized in different dots, and we believe it is now more clear that it shows a characteristic p-like behavior, in agreement with our identification of this transition. Notably, the cleanest p-type character of the X^{*+} transition is seen when detecting the magneto-PLE spectra at the X^{+*} emission line [Figs. 2(d)–2(f) of the Supplemental Material [40]].

For the p shell, we found that the BE of a p-shell exciton to the s-shell hole is about $\Delta_{pp} \approx 10$ meV for the studied dot. Consequently, we found that the BE of the positively charged exciton, defined as the energy difference between the charged and neutral complexes occupying the s- and p-shell levels, increases more than 2 times from the p-shell to the s-shell complex (the Δ_{pp}/Δ_{ss} ratio equals about 2.5).

Our experimentally obtained value of the R ratio, $\approx$2.5, qualitatively agrees with the calculations of the presented simplified model. Based on the description of the GaAlAs/AlAs dots, discussed in Refs. [23,27], we assumed that the $\omega_e + \omega_h$ value is in the range of 10–20 meV, while the ω_e/ω_h parameter is bigger than about 3. This situates these QDs in the top middle part of Fig. 2, where the BE ratio changes from 3 to 4, which is very close to the experimental value.

This result confirms the validity of the proposed model based on some very general assumptions related to the basic properties of electron-hole complexes in QDs.

V. CONCLUSIONS

We proposed a theoretical model which described the "shell" effect on the binding energy of the positively charged excitons. Our calculations showed that the BE ratio remarkably remains almost constant over a broad range of applied parameters. We performed PL and PLE excitation measurements

on the GaAs/AlGaAs QDs to verify the validity of the model. We showed that application of magnetic field was necessary to identify the excited states of both the neutral and positively charged excitonic states. Based on experimental values of the BE of the positively charged exciton we obtained qualitative agreement between the experimental results and the predictions of our theory. Our results confirm the relevance of the applied model to the description of electron-hole complexes in QDs.

ACKNOWLEDGMENTS

The authors thank K. Nogajewski for valuable discussions. The work was supported by the Foundation for Polish Science International Ph.D. Projects Programme cofinanced by the EU European Regional Development Fund. M.R.M. kindly acknowledges National Science Center (NCN) Grants No. DEC-2013/08/T/ST3/00665 and No. DEC-2013/09/N/ST3/04237 for financial support for his Ph.D. A.W. acknowledges support from the NCN under Grant No. 2014/14/A/ST3/00654.

[1] M. Grundmann, D. Bimberg, and N. N. Ledentsov, *Quantum Dot Heterostructures* (Wiley, New York, 1998).
[2] L. Jacak, P. Hawrylak, and A. Wojs, *Quantum Dots* (Springer, Berlin, 1998).
[3] *Nano-Optoelectronics Concepts, Physics, and Devices*, edited by M. Grundmann (Springer, Berlin, 2002).
[4] J.-W. Luo and A. Zunger, Phys. Rev. B **84**, 235317 (2011).
[5] Y. Benny, Y. Kodriano, E. Poem, D. Gershoni, T. A. Truong, and P. M. Petroff, Phys. Rev. B **86**, 085306 (2012).
[6] V. Mlinar, M. Bozkurt, J. M. Ulloa, M. Ediger, G. Bester, A. Badolato, P. M. Koenraad, R. J. Warburton, and A. Zunger, Phys. Rev. B **80**, 165425 (2009).
[7] M. Zieliński, K. Gołasa, M. R. Molas, M. Goryca, T. Kazimierczuk, T. Smoleński, A. Golnik, P. Kossacki, A. A. L. Nicolet, M. Potemski, Z. R. Wasilewski, and A. Babiński, Phys. Rev. B **91**, 085303 (2015).
[8] A. Wójs and P. Hawrylak, Solid State Commun. **100**, 487 (1996).
[9] S. Raymond, S. Fafard, P. J. Poole, A. Wójs, P. Hawrylak, S. Charbonneau, D. Leonard, R. Leon, P. M. Petroff, and J. L. Merz, Phys. Rev. B **54**, 11548 (1996).
[10] P. Hawrylak, Phys. Rev. B **60**, 5597 (1999).
[11] S. Tarucha, D. G. Austing, T. Honda, R. J. van der Hage, and L. P. Kouwenhoven, Phys. Rev. Lett. **77**, 3613 (1996).
[12] B. T. Miller, W. Hansen, S. Manus, R. J. Luyken, A. Lorke, J. P. Kotthaus, S. Huant, G. Medeiros-Ribeiro, and P. M. Petroff, Phys. Rev. B **56**, 6764 (1997).
[13] S. Raymond, S. Studenikin, A. Sachrajda, Z. Wasilewski, S. J. Cheng, W. Sheng, P. Hawrylak, A. Babiński, M. Potemski, G. Ortner, and M. Bayer, Phys. Rev. Lett. **92**, 187402 (2004).
[14] A. Babiński, M. Potemski, S. Raymond, J. Lapointe, and Z. R. Wasilewski, Phys. Rev. B **74**, 155301 (2006).
[15] T. Köppen, D. Franz, A. Schramm, C. Heyn, J. Gutjahr, D. Pfannkuche, D. Heitmann, and T. Kipp, Phys. Rev. B **83**, 165307 (2011).
[16] A. Wojs, P. Hawrylak, S. Fafard, and L. Jacak, Phys. Rev. B **54**, 5604 (1996).
[17] A. Wojs and P. Hawrylak, Phys. Rev. B **53**, 10841 (1996).
[18] A. Wojs and P. Hawrylak, Phys. Rev. B **55**, 13066 (1997).
[19] M. Bayer, O. Stern, P. Hawrylak, S. Fafard, and A. Forchel, Nature (London) **405**, 923 (2000).
[20] A. Trüby, M. Potemski, and R. Planel, Solid-State Electron. **40**, 139 (1996).
[21] A. Wysmołek, M. Potemski, and V. Thierry-Mieg, Physica E (Amsterdam, Neth.) **12**, 876 (2002).
[22] A. Wysmołek, B. Chwalisz, M. Potemski, R. Stępniewski, A. Babiński, and S. Raymond, Acta Phys. Pol. A **106**, 367 (2004).
[23] B. Piętka, Ph.D. thesis, Joseph Fourier University, Grenoble I, and University of Warsaw, 2007.
[24] M. Molas, K. Gołasa, B. Piętka, M. Potemski, and A. Babiński, Acta Phys. Pol. A **122**, 988 (2012).
[25] M. D. Martín, C. Antón, L. Viña, B. Piętka, and M. Potemski, Europhys. Lett. **100**, 67006 (2012).
[26] B. Piętka, J. Suffczyński, M. Goryca, T. Kazimierczuk, A. Golnik, P. Kossacki, A. Wysmolek, J. A. Gaj, R. Stępniewski, and M. Potemski, Phys. Rev. B **87**, 035310 (2013).
[27] M. Molas, Ph.D. thesis, Joseph Fourier University, Grenoble I, and University of Warsaw, 2014.
[28] M. R. Molas, A. A. L. Nicolet, A. Babiński, and M. Potemski, Europhys. Lett. **113**, 17004 (2016).
[29] T. Kazimierczuk, J. Suffczyński, A. Golnik, J. A. Gaj, P. Kossacki, and P. Wojnar, Phys. Rev. B **79**, 153301 (2009).
[30] A. Babinski, S. Awirothananon, J. Lapointe, Z. Wasilewski, S. Raymond, and M. Potemski, Physica E (Amsterdam, Neth.) **26**, 190 (2005).
[31] D. Gammon, E. S. Snow, B. V. Shanabrook, D. S. Katzer, and D. Park, Phys. Rev. Lett. **76**, 3005 (1996).
[32] I. Favero, G. Cassabois, C. Voisin, C. Delalande, P. Roussignol, R. Ferreira, C. Couteau, J. P. Poizat, and J. M. Gérard, Phys. Rev. B **71**, 233304 (2005).
[33] T. Flissikowski, A. Hundt, M. Lowisch, M. Rabe, and F. Henneberger, Phys. Rev. Lett. **86**, 3172 (2001).
[34] M. Bayer, G. Ortner, O. Stern, A. Kuther, A. A. Gorbunov, A. Forchel, P. Hawrylak, S. Fafard, K. Hinzer, T. L. Reinecke, S. N. Walck, J. P. Reithmaier, F. Klopf, and F. Schafer, Phys. Rev. B **65**, 195315 (2002).
[35] K. F. Karlsson, M. A. Dupertuis, D. Y. Oberli, E. Pelucchi, A. Rudra, P. O. Holtz, and E. Kapon, Phys. Rev. B **81**, 161307 (2010).
[36] M. R. Molas, A. A. L. Nicolet, M. Potemski, and A. Babiński, Acta Phys. Pol. A **124**, 785 (2013).
[37] T. Warming, E. Siebert, A. Schliwa, E. Stock, R. Zimmermann, and D. Bimberg, Phys. Rev. B **79**, 125316 (2009).
[38] V. Fock, Z. Phys. **47**, 446 (1928).
[39] C. G. Darwin, Proc. Cambridge Philos. Soc. **27**, 86 (1930).
[40] See Supplemental Material at http://link.aps.org/supplemental/10.1103/PhysRevB.94.235416 for the PLE spectra measured in magnetic fields on several different single QDs.
[41] Y. Benny, Y. Kodriano, E. Poem, S. Khatsevitch, D. Gershoni, and P. M. Petroff, Phys. Rev. B **84**, 075473 (2011).
[42] M. R. Molas, A. A. L. Nicolet, B. Piętka, A. Babiński, and M. Potemski, Acta Phys. Pol. A **126**, 1066 (2014).
[43] M. R. Molas, A. A. L. Nicolet, B. Piętka, A. Babiński, and M. Potemski, J. Phys. Condens. Matter **28**, 365301 (2016).